Development of Numerical Model for Simulation Intake Flow in Combustion Chamber of L-Head Engine Type

Musthafah Mohd Tahir[1], Abdul Muhaimin Mohd Shafie[1], Fudhail Abdul Munir[1], Muhammad Zahir Hassan[2]
[1]Centre for Advanced Research on Energy (CARe), Universiti Teknikal Malaysia Melaka, Malaysia
[2]Faculty of Engineering Technology, Universiti Teknikal Malaysia Melaka, Malaysia.

***Abstract*— Flow inside the combustion chamber plays the main role in the combustion process. This paper analyzed the behavior of the flow inside the L-type combustion chamber for in-cylinder engine with three different simulations. The first simulation is dealing with the static geometry of the domain. There are only combustion chambers and piston volume involved in the static simulation. The air inlet velocity is calculated using the standard engine formula for the piston at position of 9°, 18°, 27°, 36°, and 45° degrees after the top dead center. Engine speed ranges from 1500 rpm to 4500 rpm with increment of 500 rpm. The second simulation called port-flow simulation also deals with the static geometry domain but there is an addition at the intake port and intake valve. The piston volume is set to be at highest volume. There are three different valve lift used. The inplanum pressure is set to the environment pressure and the outplanum pressure is set according to the chosen values.**

***Index Term*— Micro power generation, micro-scale combustors, heat recirculation**

I. Introduction

Taking into account the global energy crisis and environmental impact of global warming, improvement of the efficiency of combustion engine is vital in this era. Fossil fuels such as gasoline and diesel are non-renewable energy which keep decreasing in this world as the demand of the energy increases over the year globally. Report from International Energy Agency (IEA) found that growths of energy demand to the year of 2040 are increasing about 37% with the average rate of growth of 1.1% per year [1]. Meanwhile, the oil demand is rising by 14mb/d to achieve 104mb/d in 2040 with China as the largest oil-consuming country despite the new policies all over the world promoting to switching the fuel and enhancing the energy efficiency [1].

Due to this limitation of fossil fuel, research has to be more profound in order to utilize the highest efficiency of the system so as to reduce the consumption of the fuel. According to Deng and Liu [2], saving one liter of gasoline can reduce the emission of carbon dioxide and carbon emission by 2.3 kg and 0.627 kg respectively. Meanwhile, saving one liter of diesel will reduce 2.63 kg of carbon dioxide along 0.717 kg of carbon.

In Malaysia, the energy consumption for oil is 32.1% which is equivalent to 83 938 kilotonne (ktoe) that is used in power plant and oil refinery. The ktoe refers to an energy unit released by the amount of 1000 tons of oil burning, which is equivalent to 42 gigajoules. Other energies include natural gas, coal, and hydro technology. Non-renewable energies are the primary energy supply in Malaysia. Total energy consumption in Malaysia in 2012 was 46 709 ktoe. Transport sector becomes the highest contributors with 17 180 ktoe, which is 36.8% of the total energy consumption [3].

Environmental issues, such as global warming, become the major factor to be focused. According to the APEC report [4], carbon dioxide emission is estimated to increase about 46% by year 2035 as compared to the year 2010. Hence, stringent legislation need to be established to control the emission. The reduction process of emission started with Euro 1 standards in 1992 involving a passenger car only.

This paper present the method of performing numerical simulation on intake flow for L-type cylinder engine using commercial Computational Fluid Dynamics (CFD) software.

II. RESEARCH APPROACH

A. *Pre-solver set-up*

1) Geometry of Computational Domain

The head of the engine was dismantled out in order to convert it to the CAD file by scanning the head method which is used by Bialy et al. [5]. Before starting the process of scanning, the domain is first affixed with the 'dot' sticker on the desired scanning surface in order to align the point in the software. After that, the surface is then covered with white color to prevent the shining surface as it will affect the precision of the process. As the scanner used a structured-light as shown in Fig.1, it is very sensitive with the reflection of the light. This type of scanner initially projects a pattern of light on the head, then it will observe the deformation of the pattern and the distance of every point is then calculated. The scanned file is then transferred to the *ezScan4.5* software in point cloud formation to reorder, align, smoothen, and delete the unwanted region within the scanned object before converting it to the *.stp* file format for geometrical model development. For this purpose, CATIA V5 software as used by Rohit and Naveen in their research [6].

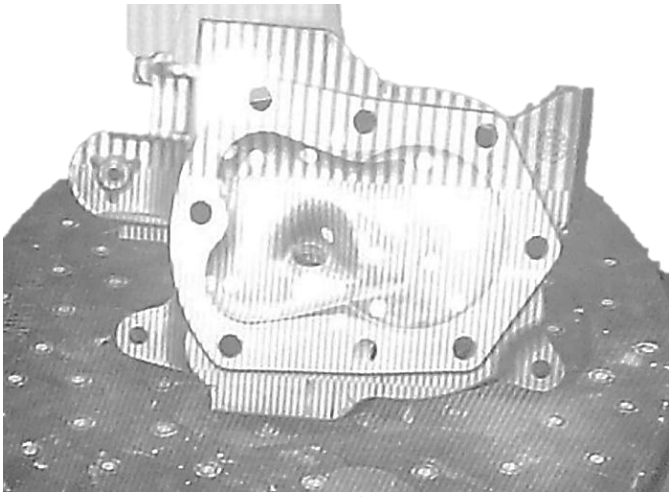

Fig. 1. Scanning of engine head

In the CATIA V5R20 software, the combustion chamber is converted to the head profile before it is assembled with other parts of the engine such engine block, intake valve, exhaust valve, and piston. The domain was created according to the actual engine as illustrated in Fig.2 with the specifications shown in the Table 1 in ANSYS Design Modeler. Three different domains need to be considered. The first domain involves no valve and the second involves the intake and exhaust valve. The addition of the intake plenum and the out plenum for second domain is needed in order to capture the boundary layer effect. The third domain is almost the same with the first domain but consists of intake and exhaust valve.

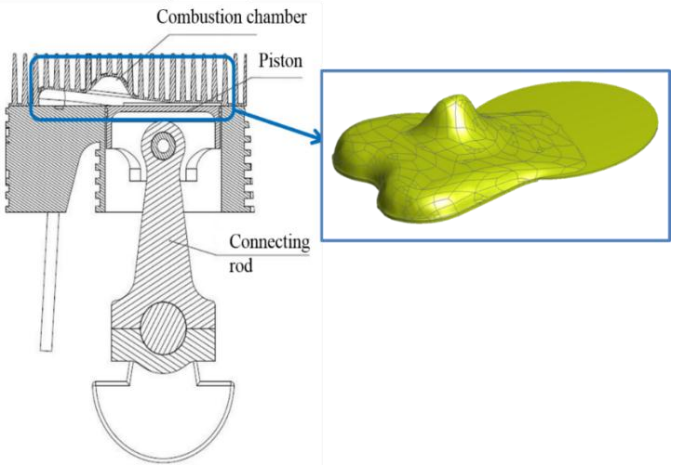

Fig. 2. Clearance volume of the in-cylinder engine and imported domain in ANSYS workbench.

Table I
Specification of engine used

Engine type	Robin EY20-3, 0.5 HP
Max. Power (HP/rpm)	5/4000
Max. Torque (Nm/rpm)	9.6/2800
Bore $\times$ Stroke (mm)	67.4 $\times$ 52
Intake air type	Naturally aspirated
Type of Piston Head	Flat
Compression Ratio	6.3
Inlet Diameter (mm)	26
Outlet Diameter (mm)	21

Fig.3 shows the first computational domain to be analyzed. Note that this computational domain is coming from an L-head type or known as Ricardo head [7]. Both valves are located on the same side of the cylinder. The cylinder head appears flat because of it contains only combustion chamber space rather than another part found in overhead valve. The disadvantage of L-head is it has low compression due to loss in the large combustion chamber.

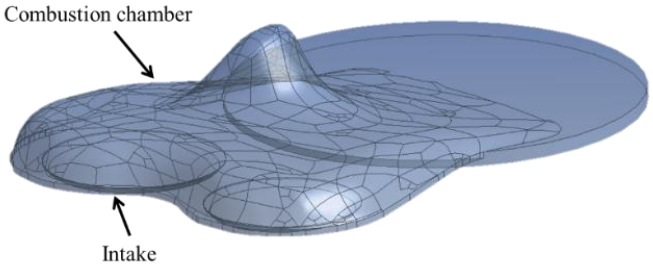

Fig. 3. Computational domain

A comprehensive study was conducted by comparing the physical model with computational model in order to minimize the modelling error with fewer numbers of iterations [8]. Fig.2 shows the domain that is imported to the ANSYS workbench while Fig.4 shows the complete cycle of a four-stroke engine. The position of the engine is varied with 9°, 18°, 27°, 36°, and 45° after top dead center. Each of the angles has different domain. The simulation runs at various speeds with increment of 500 rpm starting at 1500 rpm and ending at 4500 rpm.

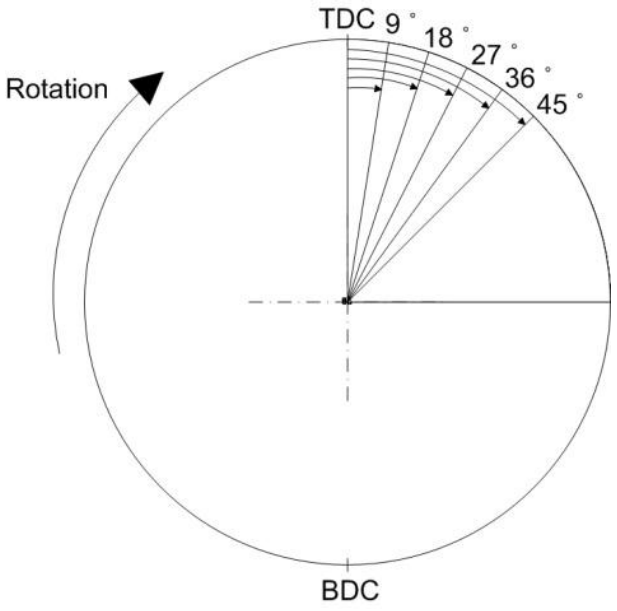

Fig. 4. Geometry is built according to desired angle.

The additions of inlet plenum for the second domain is made in order to capture the boundary layer effect at the inlet boundary condition and to create the atmosphere effect without any entrance loss as shown in Fig.5. Additions of the out plenum is to capture the stagnation pressure at the end of chamber. Furthermore, the intake valve is also included in the domain to observe the effect of valve lift towards the flow. The behavior of swirl inside the domain is monitored using three planes with locating 6 mm, 21 mm, and 46 mm downward *z*-axis. This domain is used in the Port-flow simulation with three different valve lift from low, middle, and full with values of 2.15 mm, 3.26 mm, and 6.52 mm from the valve seat. All of the domains will be consolidated to form a new single part. This is important to be done inside the design module in order to have a conformal mesh in the meshing workbench.

The option of dynamic meshing was introduced in the third domain as the intention of the simulation is to simulate the complete cycle of the four stroke engine without having the chemical reaction which called as cold–flow simulation. The imported geometry is divided into a smaller volume before meshing as intended to mesh each volume separately. Decomposition partition of volumes into sub-volumes is done and then the sub-volumes are meshed individually in order to get a good quality mesh. The piston is located at the TDC in the domain of Cold-Flow before it is divided into small volumes. The domain comprises of six multi parts and four single parts that have been decomposed into small volume to refine the geometry as shown in Fig.6. Hence, the meshing will be time efficient and easy to do according to the desired meshing type. When the valve is at closed position, minimum valve lift between the valve and valve seat is compulsory as the valve is not completely closed. This is to ensure that the gap between the valve and valve seat will not disappear. Minimum value required between the valve and valve seat is in the range of 0.05 mm to 0.5 mm since dynamic mesh problems require at least one layer remains in order to avoid the cell from being degenerated. Furthermore, it is also to avoid negative volume problem that cause a flat cell existence which will lead to the convergence problem when the solution is updated for the next step.

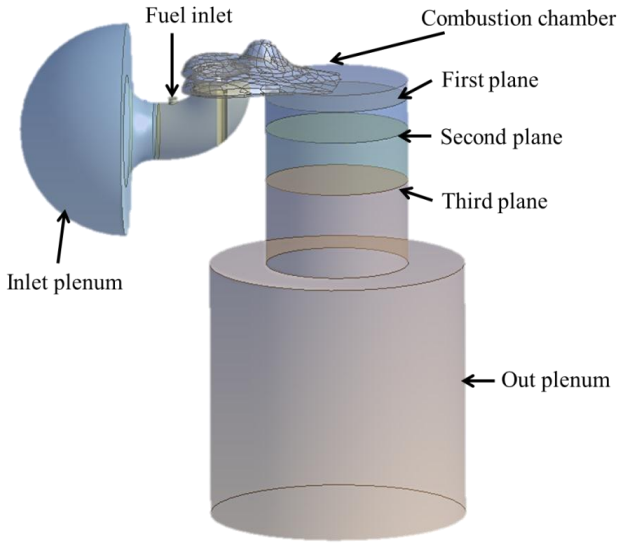

Fig. 5. Port-flow domain

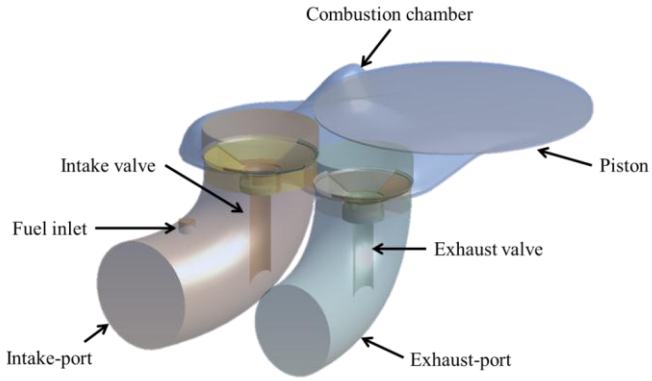

Fig. 6. Cold-flow domain.

Dealing with the dynamic simulation, valve lift profile of the engine needs to be measured before it is used in the simulation parameters. The valve lift profile is measured using the dial gauge and 360^{o} printed protractor. Fig.7 shows the valve lift profile versus crank angle that has been measured with the dial gauge. Note that the graph starts from the combustion stroke followed by exhaust, intake and compression stroke. These valve profiles will be the input value for the simulation at FLUENT [9] in the next process.

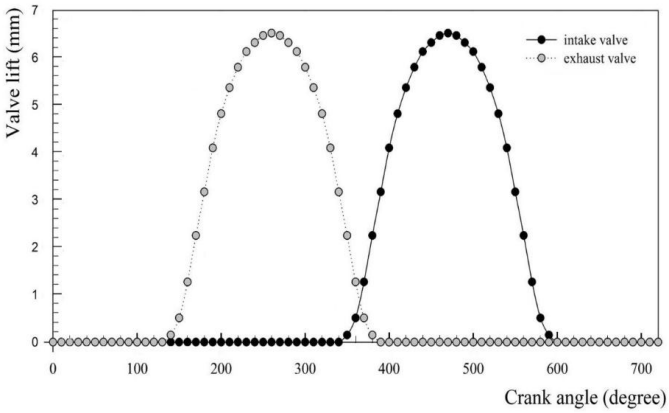

Fig. 7. Valve lift versus crank degree

2) Meshing for Steady State Simulation

In order to execute a CFD analysis, the domain is first divided into cells that form a computational mesh. ANSYS Fluent can create several types of meshes in two-dimensional and three-dimensional simulations. Tao and Satbir [10] reported that the computational mesh significantly influences the simulation result. In this study, only a three-dimensional simulation is considered. Hence, tetrahedral, wedge/prism, hexahedral, pyramid, and polyhedral cell can be used to create the domain meshing. Setup time, computational expense, and numerical diffusion are three major factors need to be taken into account in creating the mesh of the domain [11]. Quadrilateral and hexahedral cell are preferred to use when computational expense becomes a factor to monitor compared to triangular and tetrahedral cells. This is because the advantage of quadrilateral and hexahedral cells is their large aspect ratio. On the other hand, triangular and tetrahedral produce a high aspect ratio that leads to skewness. Therefore, this may cause problems in accuracy and convergence. Meshing using quadrilateral and hexahedral cells reduces the number of cells compared to triangular and tetrahedral cell.

It is preferable to have a structured mesh as it leads to better numerical properties such as quadrilateral and hexahedral mesh, but the complexity of computational domain also needs to be considered. When the mesh has better resolution, the numerical diffusion influences are also better. Mesh quality is important to get an adequate accuracy and stability of the calculation. Three main mesh qualities that need monitoring for every meshing are orthogonal quality, aspect ratio, and skewness as these qualities significantly impact on the accuracy of the numerical solution. The meshing is acceptable when the aspect ratio value is lower than 10. Aspect ratio is a measure of the stretching of the cell. Its orthogonal quality is measured using the vector from the cell centroid to each of the faces in the cell. The corresponding face area vector and the vector from the cell centroid to the centroids of each of the adjacent cells are measured. Orthogonal quality approaching to 0 is the worst cell while the best cells are closer to a value of 1. Note that, it is compromising to have the minimum orthogonal quality greater than 0.01 with the average orthogonal quality of the domain is higher than 0.5.

Skewness is defined as the difference between the shape of the cell and the shape of an equilateral cell of equivalent volume. Skewness of the cell often depends on the aspect ratio of the element. Quadrilateral cell will have a vertex angle close to 90 degrees, while triangular cell preferably has angle close to 60 degrees and all angles are less than 90 degrees. The skewness quality for quadrilateral/hexahedral cell is less than triangular/tetrahedral cell. The general rule to control the skewness of the cell is by keeping the maximum skewness of the domain below 0.95, with an average value that is significantly lower. Skewness value more than 0.95 leads to difficulties to converge, decrease in accuracy and destabilization of the solution. Table II shows the skewness ranges and corresponding cell quality.

Table II
Skewness ranges and cell quality

Skewness	Cell Quality
1	Degenerate
0.9 – <1	Bad (silver)
0.75 – 0.9	Poor
0.5 – 0.75	Fair
0.25 – 0.5	Good
>0 – 0.25	Excellent
0	Equilateral

Grid independence study was carried out for each of the domain initially to find the minimum number of cell number with shorter computational time and consistent data which lead to good result before the best domain is chosen to be simulated. Meshing with coarse mesh may lead to high deviation of the results and fine mesh will lead to longer computational time [12]. Different meshing size for each model is used to study the grid independence of the domain and commonly the size of the domain is selected from the large to fine mesh size. Velocity magnitude, in-cylinder pressure, and temperature are some of the parameters that are monitored and then compared to each of the model. Fine mesh is usually used as reference value in the grid independence study.

The domains for all of the steady simulation were set to use automatic mesh as these domains only have one body to mesh. Proximity and curvature option was used in *Advance size function* to control the skewness of the domain as this domain has a lot of curve surfaces and complex edges. Domain at the position of 45° after top dead center is chosen for the mesh grid and sensitivity check. Five points were selected to monitor their velocity magnitude and compared to each other until good mesh size is procured.

The mesh quality needs to comply with the mesh metric of maximum skewness below 0.98 and the maximum orthogonal quality whose value approaching to one. Mesh skewness control is significant because it will affect not only the convergence but also the result of the simulation. The domain shown in Fig.8 illustrates the cut-view of the piston located at 45° after top dead center and it was in a good quality of mesh with maximum skewness of 0.968 and orthogonality of 0.996. The elements of the domain consist of 148852 of tetrahedron elements. In order to simulate the domain, the mesh was generated in the ANSYS-Mesh to divide the domain into small sample size. Automatic mesh generation was used for the entire domain. Quality of mesh is important for the accuracy of the result.

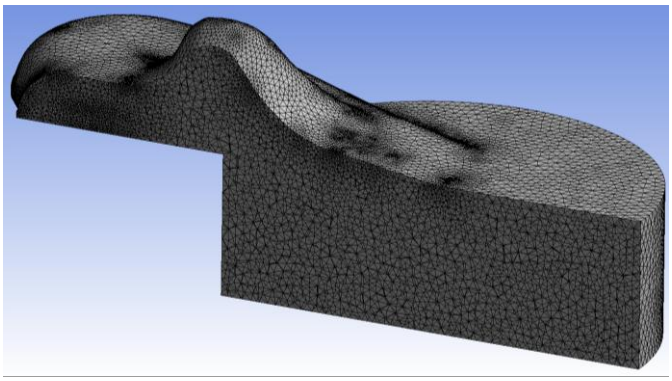

Fig. 8. Cut-view of the clearance volume of the engine.

Mesh independence study has been carried out for the domain to find out the best meshing size which produces good result. Fig.9 shows the five locations that have been selected to monitor the parameters of velocity magnitude inside the domain. Four different mesh sizes modelled from number 1 to number 4 with the mesh cells of 684000, 729000, 807000 and 824000 respectively. The velocity magnitude at chosen locations inside the domain was obtained and compared to other models as shown in the Fig.10. There is no significant variation between model three and model four. The velocity magnitude for model one and model two was compared with that for model four, the result shows a higher percentage error which is above 6%. Meanwhile the maximum percentage error for model three and model four for the velocity magnitude is only 5.3%. Considering the computational time and computer memory requirement, the mesh size for model three was used for the present study.

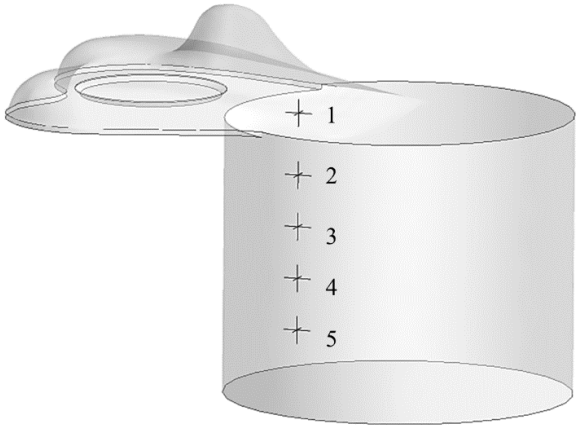

Fig. 9. Location of velocity magnitude measured.

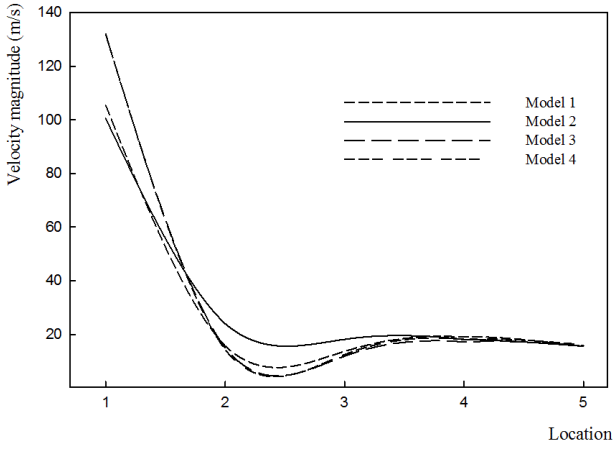

Fig. 10 Velocity magnitudes for various mesh size at chosen location.

B. *Solver Set-Up*

This simulation is performed at steady state with pressure-based solver that solves the equation of energy, momentum, and continuity at initial condition. Flow development and decay in the cylinder is usually analyzed with stable turbulence models such as k-epsilon and RNG in the CFD. Stefano et al. [13] stated that instead of using the simple model, it is recommended to use a more refined model such as Large Eddy Simulation (LES) or Detached Eddy Simulation (DES). A simple geometry is recommended to get a better RANS modelling which its Reynolds Stress and K-omega SST are enough in resolution for near wall flow.

Considering the complexities of the domain, model of Realizable k-epsilon with Non-equilibrium wall function has been used since the model is simple and stable for initial simulation strategy to predict the flow pattern in the cylinder [13]. The purpose of using Non-equilibrium wall function is to indicate the flow near the wall as the source of the turbulence and vorticity [14]. Realizable k-epsilon model handles flows involving swirl better than standard k-epsilon model [11].

Pressure field is obtained using the SIMPLE algorithm for pressure-velocity coupling. The discretization scheme for a convective term of momentum and energy uses the second order upwind scheme while the others use the first order upwind. Only two boundary conditions considered in this case; velocity inlet and pressure outlet. The other region is prescribed as wall and assumed as no-slip and adiabatic. The velocity of the inlet is calculated from the continuity of the piston speed at various engine speeds which are at 1500 rpm, 2000 rpm, 2500 rpm, 3000 rpm, 3500 rpm, 4000 rpm, and 4500 rpm.

In the viscous model option, Realizable k-epsilon with two-equation is chosen while other setting is left with the default setting. The model of Realizable k-epsilon was chosen due to its much better performance than Standard k-epsilon model for flows. This is because this model is more accurate compared to Standard k-epsilon model fin term of separation, transition, and wall impingement. One of the advantages of the k-omega model is it is suitable for complex shear flows involving rapid strain, moderate swirl, and local transition flows [14]. The advantage of Realizable k-epsilon model is it predicts the spreading rate of both planar and round jets accurately. Furthermore, it also provides the best performance for flows involving rotation, separation, and recirculation compared to Standard k-epsilon model. Meanwhile, the other option in the material properties is left with default setting.

The operating pressure is represented by the absolute pressure datum in which all relative pressure is measured. The value for pressure that is specified at the boundary condition and initial condition is related to the operating pressure. Operating pressure for Port-flow analysis is specified as the atmospheric pressure which is 101325 Pa with intention to avoid problems with round-off error which occur when the dynamic pressure differences in a fluid are small compared to the absolute pressure.

Inplenum is set as pressure-inlet in the boundary condition drop down list with gauge pressure at 0 Pa and temperature at 300 K. The flow direction is normal through the wall. The pressure-inlet option is suitable for both compressible and incompressible flows. The turbulence specified method is used with the setting of intensity and hydraulic diameter with the value of 2% and 200 mm respectively. Meanwhile, for the outplenum, it is set as the pressure-outlet in the type option in the drop-down list. The gauge pressure is set at -13172 Pa and the temperature is set at 300 K while the direction of the flow is normal to the boundary. The outlet pressure used is the same pressure as utilized in simulations reported by Shafie et al. [15].

The fuel is used in this simulation where gasoline and methane are entered the combustion chamber through the fuel inlet. The mass faction for each of the species is inserted at the inplanum, fuel inlet and outplanum. The mass fraction for fuel is set to 1 for each of the fuel type under the species mass fraction at the fuel inlet. Meanwhile, at the inplanum, the oxygen gas and nitrogen gas mass fraction is set to 0.22 and 0.74 respectively according to the standard air composition.

III. RESULTS AND DISCUSSION

The results consist of Plane A-A and Plane B-B as shown in Fig.11(a) and 11(b) to ensure the comparison legitimacy which is best done at the similar place. Plane A-A is illustrated in cutaway view in the clearance volume from the viewed from x-direction. Plane A-A which is located at the bottom surface of the combustion chamber is chosen in order to monitor the velocity profile when air enters the cylinder. Plane B-B is placed near to the flow entering the spark plug region. Flow in the cylinder is vital to the internal combustion engine to be more efficient. Swirl and tumble flow in the cylinder are inherently decisive for the mixture to be mixed well to form homogeneous mixture in a brief time before the combustion occurs. Fig.11(a) shows the flow viewed from the plane A-A located at the entering region of the flow from the combustion chamber to the swept volume. It is clearly shown that the velocity of the flow is higher at the entering region of the flow compared to the swept volume segment.

The flow velocity seems to be higher through the volume of the lower cross sectional area as manifested in the illustration of the domain. For engine speed at 4500 rpm, it is clear that the air flow velocity is higher at the left side of the wall since the inlet air located more at the left side hence producing higher velocity. It is noticeable that each of the crank angles has different values of legend at plane A-A as shown in the Fig.12(a) and 12(b). However, the maximum value for the legend at each crank angle is based on the local value at that position. Air flow at engine speed of 4500 rpm and crank angle of 45 degrees has higher velocity produced compared to the others as the inlet velocity for this circumstance is the highest. Hence, the velocity produced at this condition is the highest as well.

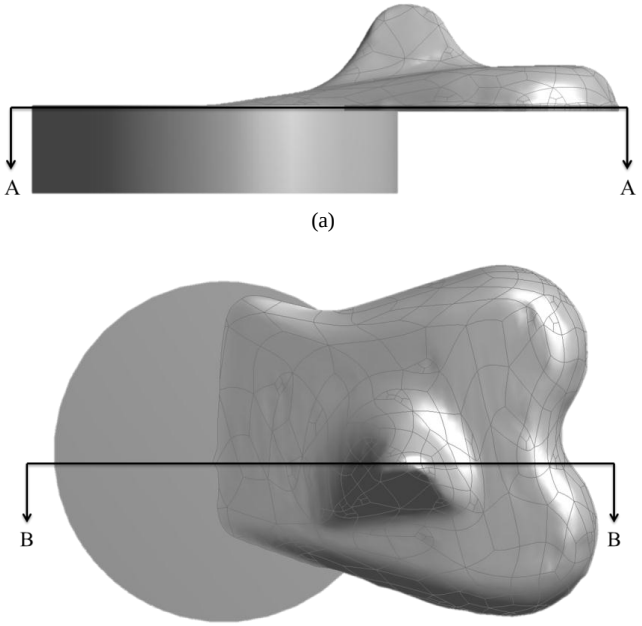

Fig. 11. (a) Reference plane of cutaway A-A; (b) Reference plane of cutaway B-B.

Legend rpm	9°	18°	27°
	Velocity (Projection) Vector 1 4.241e+001 3.181e+001 2.120e+001 1.060e+001 0.000e+000 [m s^-1]	Velocity (Projection) Vector 1 8.130e+001 6.097e+001 4.065e+001 2.032e+001 0.000e+000 [m s^-1]	Velocity (Projection) Vector 1 1.241e+002 9.308e+001 6.205e+001 3.103e+001 0.000e+000 [m s^-1]
1500			
2000	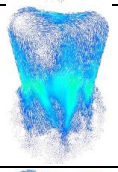		
2500	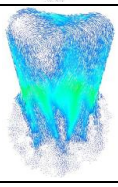	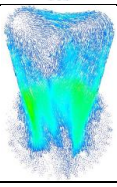	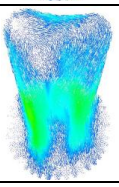
3000	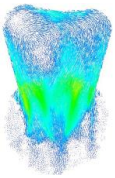	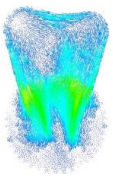	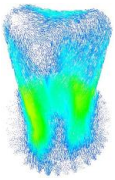
3500	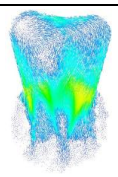	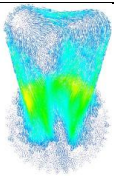	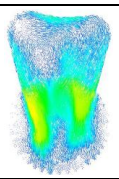
4000	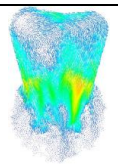	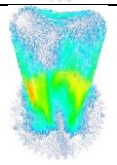	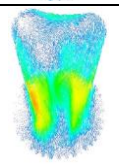
4500	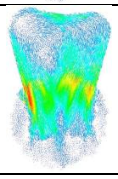	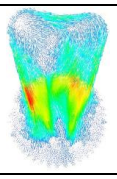	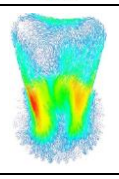

Fig. 12(a) Flow viewed from Plane A-A (9°, 18° and 27°)

Legend rpm	36°	45°
	Velocity (Projection) Vector 1 1.589e+002 1.192e+002 7.945e+001 3.972e+001 0.000e+000 [m s^-1]	Velocity (Projection) Vector 1 1.876e+002 1.407e+002 9.378e+001 4.689e+001 0.000e+000 [m s^-1]
1500		
2000		
2500	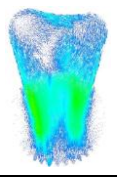	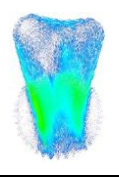
3000	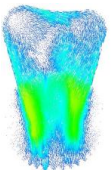	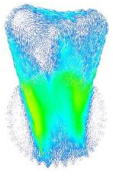
3500	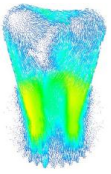	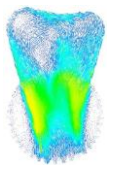
4000	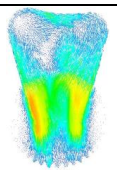	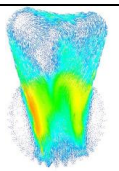
4500	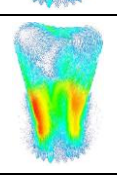	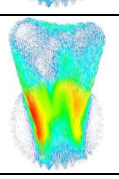

Fig. 12(b) Flow viewed from Plane A-A (36° and 45°)

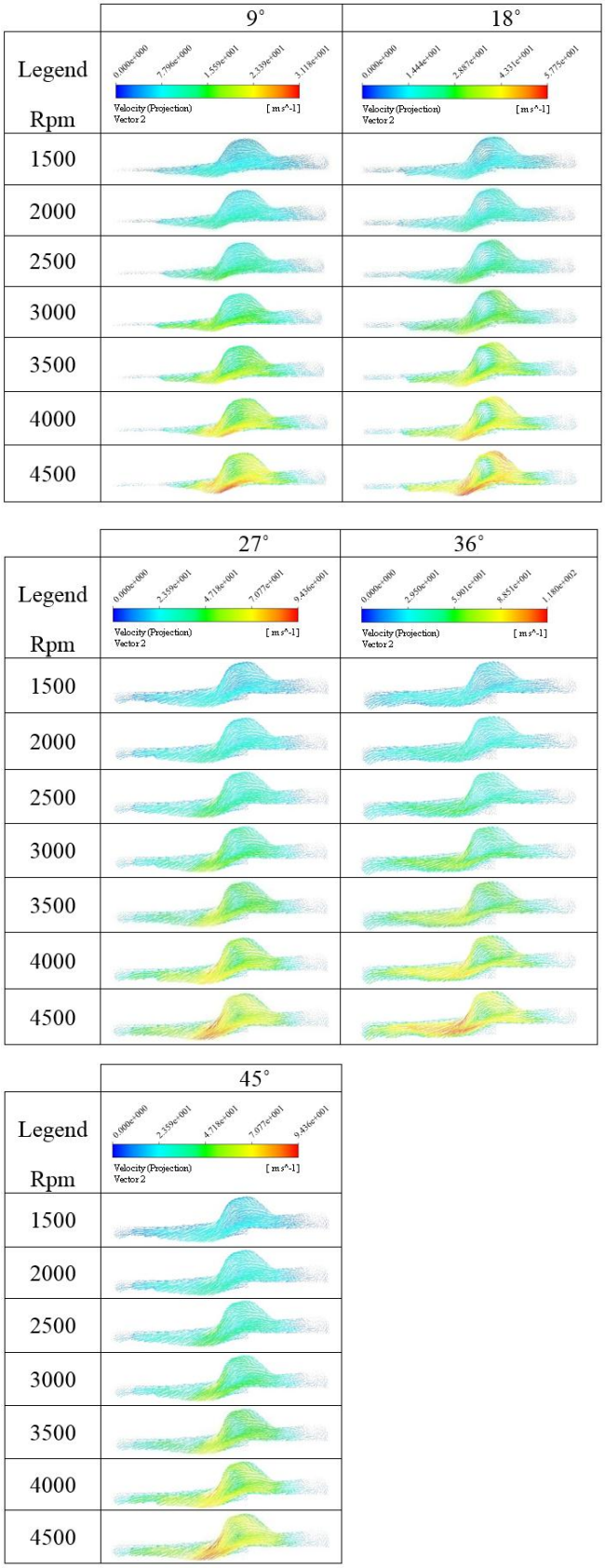

Fig. 13 Flow viewed from Plane B-B for 9˚, 18˚, 27˚, 36˚ and 45˚.

Meanwhile Fig.13 shows the view of the air flow at the Plane B-B located vertically in the cylinder and neighboring to the spark plug location. At this position, the flow of air produces around the spark plug can be observed. Most of the flows at this view have higher velocity at the entrance to swept volume, which is cylindrical as viewed from the Plane A-A. From Fig.13 as the engine speed is at 4500 rpm, at the position of piston located 18 degrees after top dead center, the flow develops high velocity close to ignition region. This can be one of the triggers of producing a tumble at the combustion chamber. Among all boundary conditions given, engine speed of 4500 rpm and crank angle of 45 degrees creates highest velocity at the entrance of swept volume which later produces swirl and tumble. Conclusively, enhanced mixing of the fuel and air improves the engine performance. High engine speed produces a high inlet air flow which helps the development of higher swirl and vice versa.

The flow structure and pattern of air inside the swept volume for a steady state condition with desired parameters given are shown in the above figure. The presence of swirl and tumble inherently improves the combustion propagation hence increasing the performance of the engine. The result of the in-cylinder flow for the first 45 degrees after top dead center shows that it has higher velocity when approaching the entrance of swept volume. The flow of air during the intake process dictates the tumble and swirl formation before the piston moves upward to top dead center in compression process. It is confirmed that the turbulence occurs at the clearance volume as the shape of the squish area encourages the turbulence flow for the domain. The limitation of this paper is that the simulation is done only for the intake process and not for the compression process which can illustrate more behavior of tumble and swirl flow. For the future work, the simulation will be performed with the presence of fuel and air to observe the mixing process occurring in the clearance volume and swept volume.

IV. CONCLUSION

The numerical model for simulation of intake flow for L-Head engine type has been successfully demonstrated. For the first case, it can be concluded that the flow velocity inside the combustion chamber and cylinder increases as the intake velocity increases until the piston reaches its top velocity at 45 degrees. There is no restriction on the flow through the domain. The second case proves that the mass flow rate and velocity across the cylinder surface increase when the valve opens at the largest capacity. Meanwhile, the pressure difference at the intake port and cylinder is reduced as soon as the valve opening area increases. The swirls are high at plane close to the air entering region at the cylinder.

ACKNOWLEDGMENT

The authors would like to thank Ministry of Higher Education Malaysia and Universiti Teknikal Malaysia Melaka for the research funding (PJP/2016/FKM-CARE/S01505).

REFERENCES

[1] IEA, 2014. World Energy Outlook (2014). International Energy Agency, London

[2] Deng, Y., and Liu, Z., (2013). Fourth International Conference on Digital Manufacturing and Automation, Research of Internal Combustion Engine with Timely Adjustable Displacement.

[3] Energy Commission (2014). *Malaysia Energy Statistics Handbook 2014: Energy Indicators.* Available from http://www.meih.st.gov.my/documents/10620/adcd3a01-1643-4c72-bbd7-9bb649b206ee [Accessed 2 March 2015].

[4] APEC, (2013). Energy Demand and Supply Outlook 5th Edition, Singapore

[5] Bialy, M., Wendeker, M., Magryta, P., Czyz, Z. and Sochaczewski, R., (2014). CFD Model of The Mixture Formation Process of the CNG Direct Injection Engine. SAE Technical Paper.

[6] Rohit, S., and Naveen, P., G., V., Cold Flow Simulation in an IC Engine. International Research Journal of Engineering and Technology, 2(7),pp. 82-87

[7] Roger, B., (2014). Engine Technology for The Modern World, Cheshire SK10 5DN: AJ6 Engineering

[8] Jawali, M. M., Kumar, D., Ramachandra, Y. B., (2013). In-Cylinder Flow Analysis in a Two-Stroke Engine- A Comparison of Different Turbulence Models Using CFD. SAE Technical Paper. 2013-01-1085

[9] Krishna, S. A ANSYS, Academic Research, 2015. Release 16.0, Help System, Canonsburg: ANSYS, Inc.

[10] Tao, F., and Satbir, S., (2015). Predictive of Flow Separation at the Valve Seat for Steady-State Port-Flow Simulation. Journal of Engineering for Gas Turbine and Power,137 (111512).

[11] Linnea, J., and Josefin, L., (2013). An Investigation of the Dynamic Characteristics of a Tilting Disc Check Valve Using CFD Analyses, Chalmers University of Technology.

[12] Munir, F. A. and M. Mikami (2015). A numerical study of propane-air combustion in meso-scale tube combustors with concentric rings, Journal of Thermal Science and Technology 10(1): 1-12.

[13] Stefano F., Giuseppe C. & Elena S. (2013). Analysis of turbulence model effect on the characterization of the in-cylinder flow field in a HSDI diesel engine. SAE Technical Paper. 2013-01-1107.

[14] ANSYS® Academic Research, R. (2012). ANSYS® Academic Research, Release 14.0. A. Inc. Canonsburg,PA.

[15] Shafie, A., M., M., Musthafah, M., T., Ali, M., S., Rosli, A., B., Arifin, Y., M., (2015). Intake Analysis on Four-Stroke Engine Using CFD. Journal of Engineering and Applied Sciences, 10 (17), pp. 7799 – 7804